

Transcriptional response of *Candida albicans* to *Pseudomonas aeruginosa* in a polymicrobial biofilm

Ruan Fourie,¹ Errol D. Cason,² Jacobus Albertyn,¹ and Carolina H. Pohl^{1*}

¹Department of Microbial, Biochemical and Food Biotechnology, University of the Free State, Bloemfontein, 9301, South Africa

²Department of Animal Wildlife and Grassland Sciences, University of the Free State, Bloemfontein, 9301, South Africa

*Corresponding author: Department of Microbial, Biochemical, and Food Biotechnology, Swot Road C/o Dekaan and Jool Street, University of the Free State, 205 Nelson Mandela Drive, Park West, Bloemfontein 9301, South Africa. PohlCH@ufs.ac.za

Abstract

Candida albicans is frequently co-isolated with the Gram-negative bacterium, *Pseudomonas aeruginosa*. *In vitro*, the interaction is complex, with both species influencing each other. Not only does the bacterium kill hyphal cells of *C. albicans* through physical interaction, it also affects *C. albicans* biofilm formation and morphogenesis, through various secreted factors and cell wall components. The present study sought to expand the current knowledge regarding the interaction between *C. albicans* and *P. aeruginosa*, using transcriptome analyses of early static biofilms. Under these conditions, a total of 2,537 open reading frames (approximately 40% of the *C. albicans* transcriptome) was differentially regulated in the presence of *P. aeruginosa*. Upon deeper analyses it became evident that the response of *C. albicans* toward *P. aeruginosa* was dominated by a response to hypoxia, and included those associated with stress as well as iron and zinc homeostasis. These conditions may also lead to the observed differential regulation of genes associated with cell membrane synthesis, morphology, biofilm formation and phenotypic switching. Thus, *C. albicans* in polymicrobial biofilms with *P. aeruginosa* have unique transcriptional profiles that may influence commensalism as well as pathogenesis.

Keywords: *Candida albicans*; *Pseudomonas aeruginosa*; polymicrobial biofilm; hypoxia; metal homeostasis; morphogenesis

Introduction

Interkingdom interactions are ubiquitous in nature and can affect various aspects of growth, antimicrobial resistance and virulence of species within a consortium (Polke et al. 2015). These interactions are frequently encountered in polymicrobial associations formed between the opportunistic fungal pathogen, *Candida albicans*, and commensal microorganisms as well as pathobionts in humans (Morales and Hogan, 2010; Diaz et al. 2012; Neville et al. 2015). This is, in part, due to the ability to form biofilms on both abiotic and biotic surfaces (Polke et al. 2015). This facilitates physical interaction, interaction with various secreted molecules and competition for nutrients (De Sordi and Mühschlegel 2009; Elias and Banin 2012).

C. albicans is frequently co-isolated with the Gram-negative bacterium, *Pseudomonas aeruginosa* (Haiko et al. 2019). *In vitro*, the interaction is complex, with both species influencing each other (Fourie and Pohl 2019). The bacterium was found to lyse and kill hyphal cells of *C. albicans* through physical interaction (Hogan and Kolter 2002; Brand et al. 2008; Bandara et al. 2010). In addition, it affects *C. albicans* biofilm formation and morphogenesis, through various secreted factors and cell wall components (Hogan et al. 2004; McAlester et al. 2008; Bandara et al. 2010, 2013; Holcombe et al. 2010). This includes inhibition of morphogenesis from yeast to hyphal morphologies by phenazines, quorum sensing molecules, lipopolysaccharides, and via sequestration

of iron, as well as promotion of morphogenesis by peptidoglycan. These stimuli elicit their effects through various signaling pathways in *C. albicans* (Shareck and Belhumeur 2011). Therefore, multiple stimuli, occurring simultaneously, from co-incubation with *P. aeruginosa* may play a role to affect the morphology of *C. albicans*. This research entailed a deeper look into the interaction between *C. albicans* and *P. aeruginosa* in polymicrobial biofilms, using RNAseq, with a focus on the transcriptional response of *C. albicans*.

Materials and methods

Strain maintenance

C. albicans SC5314 was stored at -80°C with 15% glycerol. Yeast strains were revived and maintained on yeast malt (YM) agar (3 g l⁻¹ malt extract, 3 g l⁻¹ yeast extract, 5 g l⁻¹ peptone, 10 g l⁻¹ glucose, 16 g l⁻¹ agar) at 30°C. *P. aeruginosa* PAO1 was stored at -80°C with 25% glycerol and revived and maintained on Luria-Bertani (LB) agar (5 g l⁻¹ yeast extract, 10 g l⁻¹ tryptone, 10 g l⁻¹ sodium chloride, and 15 g l⁻¹ agar).

Mono- and poly-microbial biofilm formation

Formation of biofilms were adapted from previous studies (Ells et al. 2011; Fourie et al. 2017). For monomicrobial biofilm formation, *C. albicans* was grown on YM agar for 24 hours at 30°C, inoculated into 10 mL yeast nitrogen base (YNB) broth (10 g l⁻¹

Received: November 08, 2020. Accepted: February 05, 2021

© The Author(s) 2021. Published by Oxford University Press on behalf of Genetics Society of America.

This is an Open Access article distributed under the terms of the Creative Commons Attribution License (<http://creativecommons.org/licenses/by/4.0/>), which permits unrestricted reuse, distribution, and reproduction in any medium, provided the original work is properly cited.

glucose, 6.7 g l⁻¹ YNB) and incubated at 30 °C for 24 hours. Cells were harvested (1,878 × g, 5 minutes) and the supernatant removed. This was followed by washing the cells twice with phosphate buffered saline (PBS) (Oxoid, England). The cells were counted with a hemocytometer and diluted to 1 × 10⁶ cells/mL in 20 mL filter sterilized (0.22 μm nitrocellulose filter, Merck Millipore, Ireland) RPMI-1640 medium (Sigma-Aldrich, USA). Standardized cell suspensions were dispensed into 90 mm polystyrene petri dishes (Merck, Germany), covered with Parafilm[®] and incubated for 6 hours at 37 °C to allow biofilm formation.

For polymicrobial biofilm formation, *P. aeruginosa* was grown on LB plates for 24 hours at 37 °C. Cells were inoculated into 5 mL nutrient broth (1 g l⁻¹ malt extract, 2 g l⁻¹ yeast extract, 5 g l⁻¹ peptone and 8 g l⁻¹ sodium chloride) and incubated at 37 °C for 24 hours with shaking (150 rpm). These cells were washed three times with PBS and diluted to an optical density (OD₆₀₀) of approximately 0.05 in RPMI-1640 medium containing 1 × 10⁶ cells/mL *C. albicans* and biofilms grown as described in above. Both mono- and poly-microbial biofilms were prepared and visualized with scanning electron microscopy as described in [Fourie et al. \(2017\)](#).

Total RNA extraction

Biofilms were scraped off and centrifuged (1,971 × g, 3 minutes at 4 °C). A total of five biofilms were pooled per sample. This was done in triplicate for both mono- and poly-microbial biofilms. Supernatant was aspirated from mono- and poly-microbial biofilms and 2 mL RNAlater[®] (Qiagen) added to prevent RNA degradation before storage at -80 °C. Stored biofilms samples were thawed on ice and centrifuged at 4,000 g for 5 minutes. RNAlater[®] was aspirated, and total RNA extraction was carried out using the RNeasy protect mini kit (Qiagen). At the same time, the DNA present was removed with RNase-Free DNase Set (Qiagen), according to the manufacturer's instructions. The quality of RNA in each sample was determined before sequencing at the Centre for Proteomic and Genomic Research (CPGR, Cape Town, South Africa). Quality tests carried out include checking for contaminants with the use of the NanoDrop ND1000, determining absolute concentration using the Qubit[®] RNA HS Assay Kit, as well as evaluating the integrity using the Agilent Bioanalyzer Nano Assay. A total of 1 μg of RNA per sample was treated with the Illumina Ribo-Zero rRNA Removal Kit to remove ribosomal RNA. After ribosomal RNA removal, samples were purified (Agencourt RNAClean XP Kit, Beckman Coulter) and indexed libraries were prepared using the ScriptSeq[™] v2 RNA-Seq Library Preparation Kit and ScriptSeq[™] Index PCR Primers—Set 1 (Illumina). The sizes of the libraries were profiled with the Bioanalyzer High Sensitivity Assay Kit (Agilent) and quantified (Qubit[®] HS DNA Assay Kit). Samples were diluted and a 1% Phix control library (Illumina) was spiked into samples. Sequencing was completed on the Nextseq 500 (Illumina) using Nextseq 500 High Output (150 cycle) Kit.

Analysis of differentially expressed genes

The resultant fastq files were analyzed for quality by FastQC (v0.11.5; [Andrews 2010](#)) and low-quality reads and bases were discarded using PRINSEQ-lite (v0.20.4; [Schmieder and Edwards 2011](#)). *C. albicans* samples (monomicrobial and polymicrobial) were aligned to the *C. albicans* SC5314 genome (assembly 21; The Candida Genome Database; [Skrzypek et al. 2017](#)) via TopHat2 ([Trapnell et al. 2012](#); [Kim et al. 2013](#)) using the fr-secondstrand option, which gave the best overall alignment rate ([Dutton et al. 2016](#)). Aligned files were merged with SAMtools ([Li et al. 2009](#)) and

the resultant BAM files, constructed with TopHat2, were used to construct gene expression count tables with the use of the BEDTools multicov command ([Quinlan and Hall 2010](#)). Differential expression of genes was analyzed and heatmaps and principle component analysis plots were constructed with DESeq2 ([Love et al. 2014](#)), with modified commands described at "https://gist.github.com/stephenturner/f60c1934405c127f09a6".

Determination of overrepresented functional classes of genes and transcription factors

To determine which functional classes of genes are overrepresented in our data sets, PANTHER (Protein Alignment Through Evolutionary Relationship) was utilized ([Mi et al. 2013](#); [2016](#)). Furthermore, gene lists of differentially expressed genes were evaluated for overrepresented transcription factors (TFs) using Pathogenic Yeast Search for Transcriptional Regulators And Consensus Tracking (PathoYeasttract) ([Monteiro et al. 2016](#)).

Confirmation of differential expression with nCounter[®]

Confirmation of differential expression was performed using nCounter[®] with Elements[™] XT Reagents according to manufacturer's specifications ([Geiss et al. 2008](#)). A multiplexed probe library (nCounter[®] elements CodeSet) was designed with two sequence-specific probes for genes of interest. Probes were mixed with approximately 100 ng of purified total RNA and allowed to hybridize (20 hours, 67 °C). Samples were loaded on an nCounter[®] SPRINT[™] Cartridge and processed with an nCounter[®] SPRINT Profiler (NanoString Technologies, USA). Results were processed in nSolver 4.0 software. This was done for one sample of each condition.

Results and discussion

Exploratory analysis of RNAseq data

Analysis of raw data revealed excellent quality data, with approximately 92.6% of sequences having a Phred-score of above Q30. An average of 4.3% of low-quality sequences were removed, yielding an average of 126.2 × 10⁶ sequences (150 bp paired-end) per sample. These raw reads were aligned to the genome of *C. albicans* SC5314 and further evaluated for differential expression. Complete expression profiles were compared to determine overall differences. As seen in [Figure 1A](#), monomicrobial biofilms of *C. albicans* are very similar in terms of their expression profiles with low distance between replicates, compared to polymicrobial biofilms. *C. albicans* co-cultured with *P. aeruginosa* also cluster together, however, large variation is seen between replicates compared to monomicrobial counterparts. These differences in gene expression profiles are expected due to large variation in population dynamics and microcolony formation in polymicrobial biofilms ([Stacy et al. 2016](#)). The large difference between mono- and poly-microbial biofilms is apparent through the amount of significantly differentially expressed genes ([Figure 1B](#)) with a total of 2,537 open reading frames (ORFs) (with a *p*adj < 0.05) corresponding to approximately 40% of the *C. albicans* transcriptome being altered due to the presence of *P. aeruginosa* (Supplementary Table S1). Furthermore, 917 ORFs are significantly differentially expressed at a log₂fold change (L2FC) threshold of above 1 or below -1 in the presence of *P. aeruginosa* ([Figure 1C](#)).

[Grainha et al. \(2020\)](#) used previously published data to determine the interaction between *C. albicans* and *P. aeruginosa* in polymicrobial biofilms. From these data, it is evident that various

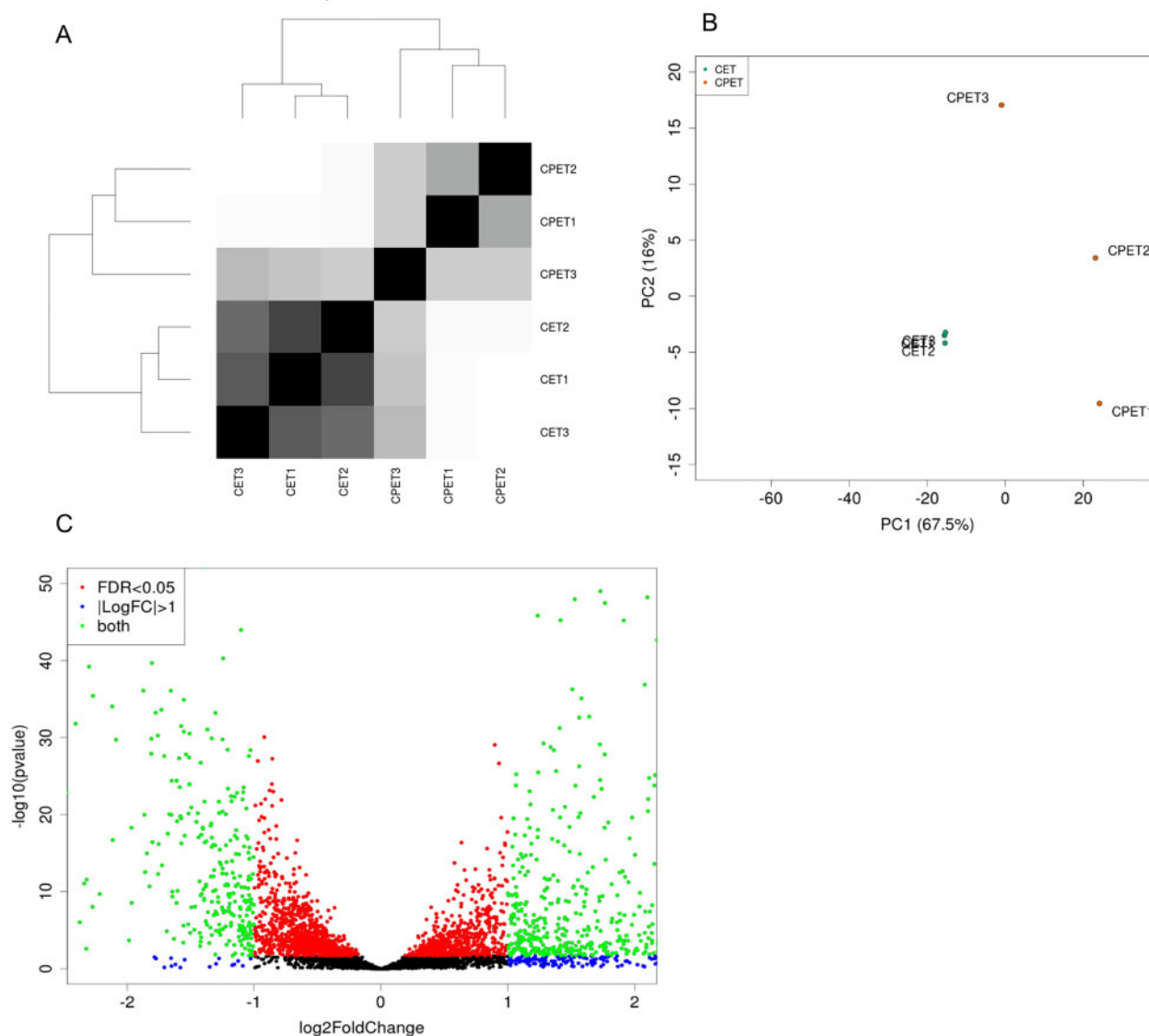


Figure 1 Distance between control and experimental biofilms using sample distance heat maps and principle component analysis plots constructed with DESeq2. (A) sample distance heat map, (B) principle component analysis plot, (C) Volcano plots of significant differentially expressed genes with $\text{Log}_{10}(\text{P-value})$ of differentially expressed genes on y-axis with the x-axis representing the log_2 fold change of these genes. Red dots indicate differential expression with a False Discovery Rate (FDR) of less than 0.05. Blue dots indicate genes that are differentially expressed with a log_2 fold change of above 1. Green represents genes adhering to both criteria. CPET—polymicrobial biofilms of *C. albicans* and *P. aeruginosa* CET—*C. albicans* monomicrobial biofilms.

different experimental approaches have been taken by researchers. When comparing our data with the most relevant high throughput experiments performed previously, we can see that in general there is little overlap between any specific data sets (Supplementary Figure S1), with no genes or proteins shared by all data sets and most being unique to a specific study. The data sets that have the most overlap with our current study is that of [Bandara et al. \(2020\)](#) for upregulated genes (22 in total) and [Trejo-Hernandez et al. \(2014\)](#) for downregulated proteins (8 in total). This lack of overlap is not surprising as there are significant experimental differences in all these studies.

Effect of *P. aeruginosa* on *C. albicans* transcriptome in early static biofilms

To determine the effect of the mentioned conditions on the transcriptome of *C. albicans*, an approach was utilized that includes

the functional analysis of gene lists to determine overrepresented functional classes of genes. It is necessary to mention that, although the functional annotation of genes is ever expanding, only a portion of *C. albicans* genes are annotated, with many genes with unknown function (as of January 27, 2020, 70.20% or 4,365 of ORFs are still uncharacterized; [Skrzypek et al. 2017](#)). Thus, the data represented here in terms of gene enrichment analysis do not incorporate many genes currently without GO annotations. Analysis of functional classes of genes that are differentially expressed in response to co-incubation with *P. aeruginosa* is given in [Table 1](#) (repressed genes) and [Table 2](#) (induced genes). For repressed genes below the Log_2FC threshold of -1 , 79 out of 264 (29.92%) genes were annotated to at least one GO term. For induced genes above the Log_2FC threshold of 1, 184 of 653 (28.18%) genes were annotated to at least one GO term. Genes associated with each GO term can be found in Supplementary Table S3.

Table 1 Overrepresented GO Terms of *C. albicans* repressed genes in response to co-incubation with *P. aeruginosa* in a polymicrobial biofilm. Over-represented Gene Ontology (GO) terms with PANTHER (Mi et al. 2013) of significantly ($p_{adj} < 0.05$) differentially expressed genes with a \log_2 fold change threshold of 1/-1. Significance based on Fisher's Exact with False Discovery Rate (FDR) multiple test correction. Unclassified indicates genes that could not be attributed to a specific GO term.

GO term	No. of differentially expressed genes	Fold enrichment	P-value	FDR
Cellular localization of products of repressed genes according to GO cellular component				
Cytosolic small ribosomal subunit (GO : 0022627)	3	24.04	0.000873	0.0157
Mitochondrial respiratory chain complex III (GO : 0005750)	3	24.04	0.000873	0.0153
Proton-transporting ATP synthase complex, catalytic core F(1) (GO : 0045261)	3	19.23	0.00137	0.0221
Proton-transporting ATP synthase complex, coupling factor F(o) (GO : 0045263)	4	12.82	0.000641	0.0118
Hyphal cell wall (GO : 0030446)	16	7.54	2.78E-09	1.07E-07
Cell surface (GO : 0009986)	26	5.02	7.59E-11	4.09E-09
Yeast-form cell wall (GO : 0030445)	8	4.75	0.000506	0.00952
Plasma membrane (GO : 0005886)	41	3.4	1.54E-11	8.91E-10
Extracellular region (GO : 0005576)	21	3.32	3.32E-06	9.94E-05
Cellular component (GO : 0005575)	174	1.26	5.94E-10	2.4E-08
Unclassified	18	0.33	5.94E-10	2.53E-08
Function of repressed genes according to GO biological process				
Cellular zinc ion homeostasis (GO : 0006882)	3	32.05	0.00051	0.02
Hydrogen peroxide catabolic process (GO : 0042744)	3	32.05	0.00051	0.0199
ATP synthesis coupled proton transport (GO : 0015986)	8	15.08	4.23E-07	4.1E-05
Tricarboxylic acid cycle (GO : 0006099)	8	12.21	1.51E-06	0.000118
Cellular iron ion homeostasis (GO : 0006879)	6	11.31	4.66E-05	0.00234
Electron transport chain (GO : 0022900)	13	7.71	7.19E-08	8.48E-06
Cellular oxidant detoxification (GO : 0098869)	6	7.69	0.000278	0.0115
Cellular response to reactive oxygen species (GO : 0034614)	5	7.28	0.00113	0.0404
Translation (GO : 0006412)	46	6.55	5.97E-23	2.6E-19
Cell adhesion (GO : 0007155)	9	3.61	0.00139	0.0488
Symbiosis, encompassing mutualism through parasitism (GO : 0044403)	13	3.39	0.000219	0.0092
Pathogenesis (GO : 0009405)	27	2.57	1.13E-05	0.000695
Response to external stimulus (GO : 0009605)	20	2.26	0.000881	0.0318
Filamentous growth of a population of unicellular organisms (GO : 0044182)	28	2.06	0.000345	0.0139
Biological process (GO : 0008150)	182	1.16	3.66E-07	3.63E-05
Unclassified	10	0.29	3.66E-07	3.71E-05

Table 2 Overrepresented GO Terms of *C. albicans* induced genes in response to co-incubation with *P. aeruginosa* in a polymicrobial biofilm. Over-represented Gene Ontology (GO) terms with PANTHER (Mi et al. 2013) of significantly ($p_{adj} < 0.05$) differentially expressed genes with a \log_2 fold change threshold of 1/-1. Significance based on Fisher's Exact with False Discovery Rate (FDR) multiple test correction. Unclassified indicates genes that could not be attributed to a specific GO term.

GO term	No. of differentially expressed genes	Fold enrichment	P-value	FDR
Cellular localization of products of repressed genes according to GO cellular component				
Membrane raft (GO : 0045121)	6	10.76	8.6E-05	0.0058
Anchored component of membrane (GO : 0031225)	23	5.05	2.12E-09	4.28E-07
Cell surface (GO : 0009986)	31	4.02	4.41E-10	1.19E-07
Extracellular region (GO : 0005576)	35	3.71	2.09E-10	8.44E-08
Fungal-type cell wall (GO : 0009277)	21	3.2	8.29E-06	0.000745
Plasma membrane (GO : 0005886)	40	2.22	4.6E-06	0.000465
Macromolecular complex (GO : 0032991)	20	0.47	7.33E-05	0.00539
Function of repressed genes according to GO biological process				
Xenobiotic transport (GO : 0042908)	4	21.51	0.000232	0.0361
Organic hydroxy compound transport (GO : 0015850)	6	10.76	8.6E-05	0.0156
Drug export (GO : 0046618)	5	10.76	0.000347	0.0421
Lipid catabolic process (GO : 0016042)	9	6.45	3.88E-05	0.00995
Fatty acid biosynthetic process (GO : 0006633)	7	6.27	0.000332	0.0414
Alcohol biosynthetic process (GO : 0046165)	8	5.55	0.000254	0.0357
Adhesion of symbiont to host (GO : 0044406)	10	4.58	0.000172	0.0279
Cellular response to oxidative stress (GO : 0034599)	14	3.76	5.97E-05	0.0124
Pathogenesis (GO : 0009405)	45	2.87	8.65E-10	1.26E-06
Biofilm formation (GO : 0042710)	17	2.79	0.000276	0.0365
Carbohydrate metabolic process (GO : 0005975)	19	2.59	0.000296	0.0379
Cellular response to drug (GO : 0035690)	28	2.08	0.000415	0.0476
Oxidation-reduction process (GO : 0055114)	40	2.04	3.23E-05	0.0101
Biological process (GO : 0008150)	258	1.1	0.000238	0.0358
Unclassified	28	0.54	0.000238	0.0346

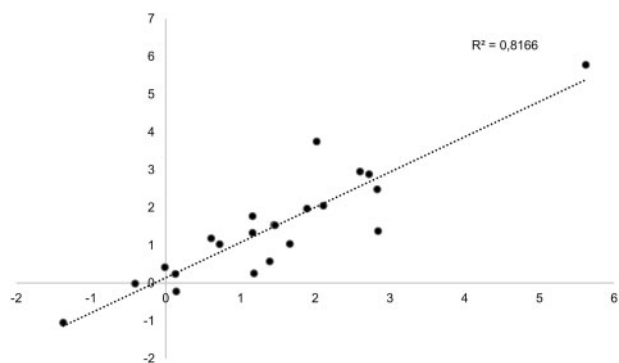


Figure 2 Correlation between Log2fold change values through Nanostring compared to RNA-Seq. Scatter plot of the Log2fold change values obtained through RNA-Seq and Nanostring of genes of interest (Supplementary Table S2) indicating the correlation between these two methods ($R^2 = 0.817$).

Confirmation of RNA-Seq data with NanoString

The fold change obtained using RNA-Seq compared with that from NanoString, using selected genes of interest is shown in Supplementary Table S2. The similarity between the transcript levels obtained from the two platforms indicates consistency in the data generated for the analysis. Figure 2 indicates the linear correlation between RNA-Seq compared to Nanostring concerning the genes in Supplementary Table S2 with a correlation coefficient (r) of 0.90 and R^2 of 0.82.

Response to low-oxygen levels

In our data set, genes involved in ATP synthesis, tricarboxylic acid cycle as well as electron transport chain are repressed. Interestingly, induction of genes related to carbohydrate metabolic process is seen. This response is expected during fermentative growth (Askew et al. 2009). In addition, several genes involved in ethanol production (*ADH5*, *ADH3*, *orf19.4504*, and *ADH2*) are induced in our data set (Supplementary Table S1). The repression of the tricarboxylic acid cycle and electron transport chain, together with the induction of the carbohydrate metabolic process and alcohol biosynthetic process may indicate that *C. albicans* relies more on fermentation for energy acquisition during co-incubation with *P. aeruginosa*.

Interestingly, genes involved in glycolysis, fermentation, stress response, cell wall, fatty acid, iron metabolism and hyphae specific genes are induced during hypoxia, whilst the tricarboxylic acid cycle, respiration and ATP synthesis are repressed (Askew et al. 2009). This response is similar to what is observed here in polymicrobial biofilms of *C. albicans* and *P. aeruginosa*, suggesting that the response of *C. albicans* toward *P. aeruginosa* may be dominated by the response toward hypoxia. The carbohydrate metabolism of *C. albicans* in a hypoxic environment is regulated by *Tye7p* and *Gal4p* (Askew et al. 2009; Bonhomme et al. 2011). Confirming our observation, is the induction of *TYE7* (Table 3) as well as *GAL4* (Supplementary Table S1), the former of which is needed for growth and virulence in a hypoxic environment.

Aerobic metabolism by *P. aeruginosa* in polymicrobial biofilms with *C. albicans* may quickly deplete available oxygen in the biofilm, forcing hypoxia quicker than in *C. albicans* monomicrobial biofilms. In addition to induced hypoxia, inhibition of *C. albicans* metabolic activity due to the production of the redox-active phenazine compounds by *P. aeruginosa*, has been reported previously (Morales et al. 2013). Morales et al. (2013) reported an increase in fermentation products, such as ethanol, by *C. albicans*,

due to the action of these phenazine compounds. Considering this, the observed effect on *C. albicans* carbohydrate metabolism may be due to not only hypoxia, but also phenazine production by *P. aeruginosa*. Interestingly, ethanol decreases *P. aeruginosa* motility and stimulates *P. aeruginosa* biofilm formation and phenazine production (Chen et al. 2014; Lewis et al. 2019).

Stress responses

GO biological process reveals a response toward stress (e.g., chemical) with response to xenobiotic as well as drug and organic hydroxy compound transport being overrepresented. This response may be due to toxic phenazines produced by *P. aeruginosa*. In addition, the cellular response to oxidative stress is overrepresented in induced genes (Table 2). The glutathione-dependent S-nitrosoglutathione reductase (encoded by *FDH3*), the nitric oxide dioxygenase (encoded by *YHB1*) as well as the transcriptional regulator (encoded by *CTA4*), playing a role in nitrosative radical detoxification, is induced in our data set (Supplementary Table S1). This may indicate a response to nitrosative stress of *C. albicans* in the presence of *P. aeruginosa* (Ullmann et al. 2004; Chiranand et al. 2008; Tillmann et al. 2015). Nitrosative radicals may be from both endogenous and exogenous origin, such as the use of nitrite as an alternative electron acceptor as well as from the redox-active phenazines produced by *P. aeruginosa* (Chiranand et al. 2008). Although the gene encoding for catalase, *CAT1*, playing a role in oxidative stress response, is repressed in our data set, the genes encoding for superoxide dismutase (*SOD*) *SOD1* and *SOD6* are significantly induced (Supplementary Table S1). *SODs* protect cells against reactive oxygen species generated by the mitochondrial respiratory chain and external sources such as the oxidative burst during phagocytosis. *SOD1* has been linked to virulence (Martchenko et al. 2004), while the function of *SOD6* still needs to be elucidated (Frohner et al. 2009). Interestingly, the mitochondrial *SOD*, encoded by *SOD2*, is not differentially regulated, indicating that the possible increase in oxidative stress is localized in the cytosol, and not due to mitochondrial activity. This may indicate that the source of oxidative stress is not due to cellular activity, but due to external factors, such as phenazines, entering the cell.

Membrane formation and organization

Lipid catabolic process, including lipase genes (*LIP1*—*LIP3*, *LIP6*, *LIP8*—*LIP10*), catalyzing hydrolysis or synthesis of triacylglycerols (Schofield et al. 2005; Gácsér et al. 2007) is overrepresented in induced genes (Table 2). In addition, fatty acid biosynthetic process is induced, possibly to counteract physical damage to *C. albicans* plasma membrane by *P. aeruginosa* (Brand et al. 2008). Importantly, several TFs, with roles in membrane and cell wall synthesis, such as *UPC2*, *STP4*, and *SUT1* are overrepresented in our data set and are significantly differentially expressed (Supplementary Table S1). In addition, *Upc2* is associated with the regulation of a hypoxic response, inducing genes involved in ergosterol biosynthesis (MacPherson et al. 2005; Synnott et al. 2010) and *Sut1p* is involved in sterol uptake during hypoxia in *S. cerevisiae* (Foster et al. 2013). Interestingly, *Sut1p* is also involved in zinc acquisition in *C. albicans* (Xu et al. 2015).

Iron and zinc homeostasis

Previous research suggests that *C. albicans* in combination with *P. aeruginosa* elicits an iron-deprivation response in *C. albicans* due to rapid iron-sequestration by *P. aeruginosa* siderophores (Singh et al. 2011; Purschke et al. 2012; Trejo-Hernández et al. 2014). This iron-deficient response is mediated by a *Cap2*-*HAP* complex, affecting

various genes including three iron uptake pathways and repression of iron utilization and storage (Singh *et al.* 2011). However, closer examination of our data revealed only a modest response toward iron deprivation in terms of repression of iron utilization genes [including *ACO1* and *IDH2* (involved in aerobic respiration), *QCR2* (respiratory electron transport chain) and haem containing proteins, like *CAT1* (hydrogen peroxide detoxification)], indicating a possible reduced dependency on iron (Table 1). This repression of iron usage genes is similar to the results obtained by Trejo-Hernández *et al.* (2014) in a proteomic study of monomicrobial and polymicrobial biofilms. None of the transcription factors (*SFU1*, *SEF1*, or *HAP43*) involved in iron regulation (Chen *et al.* 2011; Singh *et al.* 2011) was differentially regulated at 6 hours of co-incubation.

Strikingly, several genes involved in iron uptake and usage is repressed in our data set, resembling an abundance of iron compared to monomicrobial biofilms. These genes include components of the reductive iron pathway, namely those that encode the high-affinity iron permease *FTR1*, the multicopper ferroxidase *FET34*, the ferric/cupric reductase *CFL2*, the ferritin receptor *ALS3* and the heme oxygenase *HMX1*. This may indicate that less iron is required for cellular growth when *C. albicans* is co-incubated with *P. aeruginosa*, possibly due to growth repression. This contrasts with what has been reported before (Trejo-Hernández *et al.* 2014), although this may be due to differences in incubation conditions and duration of biofilm formation.

Genes involved in zinc acquisition are repressed in our data set (Supplementary Table S1), including components of a “zincophore” system, namely, the genes encoding zinc transporters (*ZRT1*, *ZRT2*, and *ZRT3*) as well as the extracellular zinc binding protein *PRA1*, responsible for zinc sequestration (Böttcher *et al.* 2015; Łoboda and Rowińska-Żyrek 2017). This “zincophore” system is under positive regulation of *Csr1p* (also known as *Zap1p*). *CSR1* is repressed in our data set, indicating that *C. albicans* is under less zinc-limitation during co-incubation with *P. aeruginosa*, similar to the effect on iron, discussed above.

Morphogenesis and biofilm formation

Scanning electron micrographs (Figure 3) indicate the attached *C. albicans* hyphae in monomicrobial and polymicrobial biofilms after 6 hours of incubation. In the polymicrobial biofilms, *P. aeruginosa* attached to the hyphae can be seen. Previous research found

that *C. albicans* morphogenesis is inhibited in the presence of *P. aeruginosa* due to the N-acyl-homoserine lactone (AHL), 3-oxo-homoserine lactone, produced by the bacterium (Hogan *et al.* 2004). *C. albicans* yeast and pseudohyphal morphologies are characterized by a morphology dependent set of expressed genes. Similarly, true hyphae formation is transcriptionally unique (Bensen *et al.* 2002) and include *HWP1*, *ECE1*, *HYR1*, *RBT1*, *RBT4*, *RBT5*, and *WAP1*, which encode GPI-modified cell wall proteins. A number of these genes, including *HWP1* and *ECE1*, are repressed in the presence of *P. aeruginosa* in our data set, associated with a predominant yeast and pseudohyphal transcriptional profile (Supplementary Table S1). In contrast, *HYR1* and *CHT2*, associated with a true hyphal-morphology, is induced in our data set.

Adhesion is a crucial component of the process of biofilm formation of *C. albicans*. In our data set, genes associated with adhesion is repressed in the presence of *P. aeruginosa* (Table 1). In addition, several TFs with roles in adhesion, including *ZFU2*, *AHR1*, and *TRY4*, are differentially regulated (Table 3). *ZFU2* and *TRY4* are TFs that regulate yeast form adherence (Böhm *et al.* 2017). However, *ZFU2* is repressed, whereas *TRY4* is induced with contrasting effects. In addition, *Ahr1p* recruits *Mcm1p* and induce initial surface adhesion during biofilm formation (Askew *et al.* 2011). Interestingly, both *AHR1* and *MCM1* are repressed in our data set. In addition, the yeast wall protein *YWP1*, whose expression negatively correlates with adhesion (Granger *et al.* 2005), is induced in response to *P. aeruginosa*, further providing evidence for an effect on adhesion.

A number of external stimuli, that may influence filamentation and biofilm formation, is found in the presence of *P. aeruginosa* (Fourie *et al.* 2016). These stimuli include hypoxia (induces filamentation), presence of LPS (represses filamentation), cell wall and membrane stress (induces filamentation), phenazines (repress filamentation) and quorum sensing molecules. It is tempting to speculate that these many stimuli may present as an exaggerated response that could be detrimental to adaptation to a host environment. Therefore, in addition to TFs, chromatin-remodeling has been shown to affect biofilm formation and filamentation through integrating signals from external stimuli and acting as a transcriptional buffer affecting transcription kinetics (Hnisz *et al.* 2010, 2012; Kim *et al.* 2012; Garnaud *et al.* 2016). The Set3/Hos2 complex (Set3C) is a NAD-dependent histone deacetylation complex [consisting of four core subunits (*Set3p*, *Hos2p*,

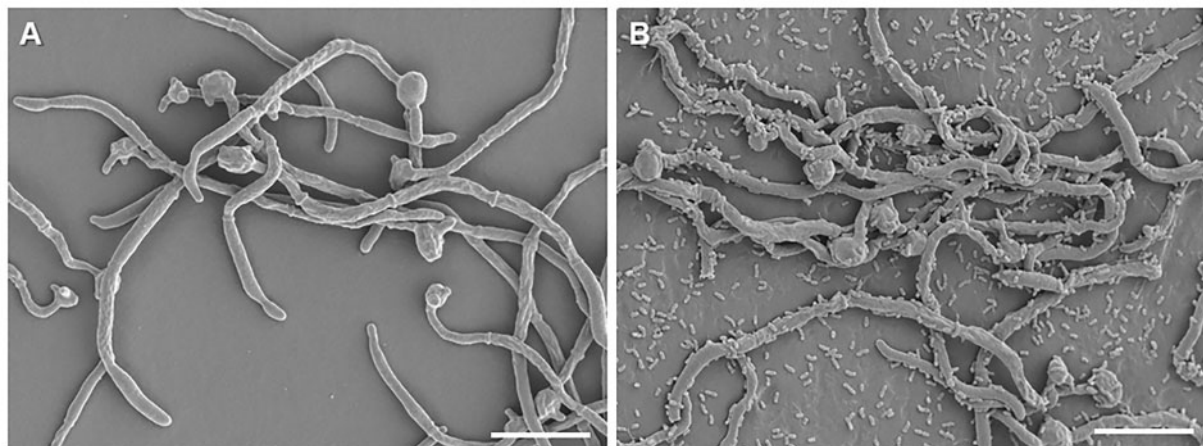


Figure 3 Scanning electron micrograph of monomicrobial and polymicrobial biofilms. (A) *C. albicans* monomicrobial biofilm, grown for 6 hours, indicating attached hyphae, (B) Polymicrobial biofilm, grown for 6 hours, indicating the attachment of *P. aeruginosa* to *C. albicans* hyphae. Scale bar represents 10 μm.

Snt1p, and Sif2p) and three peripheral subunits (Hos4p, Hst1p, and Cpr1p) (Hnisz et al. 2010)] that binds directly to most of the master regulators of biofilm formation and is involved in the dispersal of cells from mature biofilms, via the modulation of NRG1 expression levels (Nobile et al. 2014). SET3 as well as the gene encoding the peripheral subunit, HST1, is significantly induced in our data set. This raises the question if Set3C may play a role in modulating filamentation of *C. albicans* in the presence of *P. aeruginosa*, possibly inducing the dispersion of *C. albicans*, to escape the hostile activity of *P. aeruginosa* during co-incubation.

Phenotypic switching

In addition to affecting biofilm formation in *C. albicans*, the Set3C is also a regulator of white-opaque switching (Hnisz et al. 2010; Garnaud et al. 2016). Strikingly, the gene encoding the white-opaque regulator, WOR1, is induced in our data set (Supplementary Table S1). This may indicate that white-opaque switching could take place. However, WOR2 expression (required for stabilization of the opaque phenotype) is significantly repressed (Table 3), indicating that switching may be unstable and transient. In addition, whereas WH11 and EFG1 expression is associated with white-phase and OP4 and SAP1 expression is associated with the opaque phase (Tao et al. 2014), contradicting results are obtained in this data set, with both WH11 and OP4 being induced. In addition to white and opaque phenotypes, a gray phenotype can also manifest, however, comparison with expression results obtained by Tao et al. (2014) revealed little overlap between our data set and opaque or gray specific transcriptional responses. The overexpression of WOR1 in the presence of bacteria has been reported before and is required for commensal fitness (Fox et al. 2014). In these cases the full opaque program was also not induced and the authors speculate that additional signals may be required. Ramírez-Zavala et al. (2008) showed that switching could be induced in *C. albicans* by an anaerobic environment in the presence of high temperature (37 °C), however, this only occurred in the WO-1 and CAI-4 strains, and could not be replicated in the SC5314 strain that is heterozygous at the MTL(a/α). Due to this, the strain of *C. albicans* (SC5314) may experience an induction of WOR1 in the presence of *P. aeruginosa* due to hypoxia, however, the full opaque program may not be induced as a trisomy of chromosome 1 and homozygosity of the mating type locus is needed. It is however interesting to note that an increase in expression of genes encoding hydrolytic enzymes, such as SAP3 and lipases (LIP1 to LIP3, LIP6, LIP8 to LIP10), associated with the opaque phenotype (Lan et al. 2002), is seen in our data set. This provides evidence that the opaque expression profile, at least in part, may be induced by co-incubation of *C. albicans* with *P. aeruginosa*.

Conclusions

For the formation of both mono- and poly-microbial biofilms, a stationary model adapted from Fourie et al. (2017), was followed, which allows for the rapid depletion of oxygen and formation of microaerophilic to hypoxic biofilms, similar to the biofilms formed in the lungs of cystic fibrosis patients (Crocker et al. 2019). The formation of microaerophilic to hypoxic biofilms may be a more accurate representation of *in vivo* conditions, compared to planktonic growth of cells with aeration, as was previously used to determine the effect of *P. aeruginosa* on *C. albicans* (Holcombe et al. 2010). In addition, the present model also does not include a distinct adhesion phase as in many other biofilm studies. In our opinion, this also may more closely reflect *in vivo* conditions, as

biofilms involved in infection do not undergo such an initial adhesion phase and may therefore be more complex. Under these conditions, co-incubation of *C. albicans* with *P. aeruginosa* exhibited a strong response toward hypoxia, with a shift toward fermentative growth and sterol metabolism. Furthermore, the hypoxic environment may have driven the reduced expression of genes associated with iron and zinc acquisition, as hypoxia may decrease the need for these metals. Interestingly, SET3 transcription is upregulated in the presence of *P. aeruginosa*, indicating that the Set3C may be contributing to the interaction of *C. albicans* with *P. aeruginosa*, by acting as a transcriptional buffer to control yeast filamentation and dispersal. Furthermore, the white-opaque regulator, WOR1, is upregulated in the presence of *P. aeruginosa*, indicating that switching to the opaque-phenotype may be taking place, although additional signals may be required to initiate the full opaque-transcriptional profile. From these data, it is clear that these polymicrobial biofilms have a unique transcriptional profile, indicating several shifts in metabolism that may play important roles in commensalism as well as infection.

Data availability

Supplementary files for this investigation are available at figshare (<https://doi.org/10.25387/g3.13791607>). Supplementary Table S1 comprises the raw analyzed data from RNASeq experiments. Supplementary Table S2 shows a comparison between the transcripts obtained using RNA-Seq and NanoString. Supplementary Table S3 indicates the genes associated with each identified GO term. All raw data for this investigation have been deposited in the NCBI's GEO database under the accession number GSE136726.

Funding

This work was supported by the National Research Foundation of South Africa (grant number 115566 and 118543 to CHP). The funders played no role in the study or in the preparation of the article or decision to publish.

Conflict of interest: All authors declare that they have no conflict of interest.

Literature cited

- Andrews S. 2010. FastQC a quality-control tool for high-throughput sequence data. Bioinformatics doi:citeulike-article-id:11583827
- Askew C, Sellam A, Epp E, Hogues H, Mullick A, et al. 2009. Transcriptional regulation of carbohydrate metabolism in the human pathogen *Candida albicans*. PLoS Pathog. 5:e1000612.
- Askew C, Sellam A, Epp E, Mallick J, Hogues H, et al. 2011. The zinc cluster transcription factor Ahr1p directs Mcm1p regulation of *Candida albicans* adhesion. Mol. Microbiol. 79:940–953.
- Bandara HMHN, Cheung BP, Watt RM, Jin LJ, Samaranyake LP. 2013. *Pseudomonas aeruginosa* lipopolysaccharide inhibits *Candida albicans* hyphae formation and alters gene expression during biofilm development. Mol Oral Microbiol. 28:54–69.
- Bandara HMHN, Yau JYY, Watt RM, Jin LJ, Samaranyake LP. 2010. *Pseudomonas aeruginosa* inhibits *in-vitro* *Candida* biofilm development. BMC Microbiol. 10:125.
- Bandara HMHN, Wood DLA, Vanwonterghem I, Hugenholtz P, Cheung BPK, et al. 2020. Fluconazole resistance in *Candida albicans*

- is induced by *Pseudomonas aeruginosa* quorum sensing. *Sci Rep.* 10:7769.
- Bensen ES, Filler SG, Berman J. 2002. A forkhead transcription factor is important for true hyphal as well as yeast morphogenesis in *Candida albicans*. *Eukaryot Cell* 1:787–798.
- Böhm L, Torsin S, Tint SH, Eckstein MT, Ludwig T, et al. 2017. The yeast form in the fungus *Candida albicans* promotes persistence in the gut of gnotobiotic mice. *PLoS Pathog.* 13:e1006699.
- Bonhomme J, Chauvel M, Goyard S, Roux P, Rossignol T, et al. 2011. Contribution of the glycolytic flux and hypoxia adaptation to efficient biofilm formation by *Candida albicans*. *Mol Microbiol.* 80: 995–1013.
- Böttcher B, Palige K, Jacobsen ID, Hube B, Brunke S. 2015. *Csr1/Zap1* maintains zinc homeostasis and influences virulence in *Candida dubliniensis* but is not coupled to morphogenesis. *Eukaryot Cell* 14:661–670.
- Brand A, Barnes JD, Mackenzie KS, Odds FC, Gow NAR. 2008. Cell wall glycans and soluble factors determine the interaction between the hyphae of *Candida albicans* and *Pseudomonas aeruginosa*. *FEMS Microbiol Lett.* 287:48–55.
- Chen AI, Dolben EF, Okegbe C, Harty CE, Golub Y, et al. 2014. *Candida albicans* ethanol stimulates *Pseudomonas aeruginosa* WspR-controlled biofilm formation as part of a cyclic relationship involving phenazines. *PLoS Pathog.* 10:e1004480.
- Chen C, Pande K, French SD, Tuch BB, Noble SM. 2011. An iron homeostasis regulatory circuit with reciprocal roles in *Candida albicans* commensalism and pathogenesis. *Cell Host Microbe* 10: 118–135.
- Chirananand W, McLeod I, Zhou H, Lynn JJ, Vega LA, et al. 2008. CTA4 transcription factor mediates induction of nitrosative stress response in *Candida albicans*. *Eukaryot Cell* 7:268–278.
- Crocker AW, Harty CE, Hammond JH, Willger SD, Salazar P, et al. 2019. *Pseudomonas aeruginosa* ethanol oxidation by AdhA in low-oxygen environments. *J Bacteriol.* 201:e00393-19. [10.1128/JB.00393-19]
- De Sordi L, Mühlischlegel FA. 2009. Quorum sensing and fungal-bacterial interactions in *Candida albicans*: a communicative network regulating microbial coexistence and virulence. *FEMS Yeast Res.* 9:990–999.
- Diaz PI, Xie Z, Sobue T, Thompson A, Biyikoglu B, et al. 2012. Synergistic interaction between *Candida albicans* and commensal oral Streptococci in a novel *in vitro* mucosal model. *Infect Immun* 80:620–632.
- Dutton LC, Paszkiewicz KH, Silverman RJ, Splatt PR, Shaw S, et al. 2016. Transcriptional landscape of trans-kingdom communication between *Candida albicans* and *Streptococcus gordonii*. *Mol Oral Microbiol.* 31:136–161.
- Elias S, Banin E. 2012. Multi-species biofilms: living with friendly neighbors. *FEMS Microbiol Rev.* 36:990–1004.
- Ells R, Kock JLF, Albertyn J, Kemp G, Pohl CH. 2011. Effect of inhibitors of arachidonic acid metabolism on prostaglandin E₂ production by *Candida albicans* and *Candida dubliniensis* biofilms. *Med Microbiol Immunol.* 200:23–28.
- Fourie R, Ells R, Kemp G, Sebolai OM, Albertyn J, et al. 2017. *Pseudomonas aeruginosa* produces aspirin insensitive eicosanoids and contributes to the eicosanoid profile of polymicrobial biofilms with *Candida albicans*. *Prostaglandins Leukot Essent Fatty Acids* 117:36–46.
- Fourie R, Ells R, Swart CW, Sebolai OM, Albertyn J, et al. 2016. *Candida albicans* and *Pseudomonas aeruginosa* interaction, with focus on the role of eicosanoids. *Front Physiol.* 7:64.
- Fourie R, Pohl CH. 2019. Beyond antagonism: the interaction between *Candida* species and *Pseudomonas aeruginosa*. *J Fungi* 5:34.
- Foster HA, Cui M, Naveenathayalan A, Unden H, Schwanbeck R, et al. 2013. The zinc cluster protein Sut1 contributes to filamentation in *Saccharomyces cerevisiae*. *Eukaryot Cell* 12:244–253.
- Fox EP, Cowley ES, Nobile CJ, Hartooni N, Newman DK, et al. 2014. Anaerobic bacteria grow within *Candida albicans* biofilms and induce biofilm formation in suspension cultures. *Curr Biol.* 24: 2411–2416.
- Frohner IE, Bourgeois C, Yatsyk K, Majer O, Kuchler K. 2009. *Candida albicans* cell surface superoxide dismutases degrade host-derived reactive oxygen species to escape innate immune surveillance. *Mol Microbiol.* 71:240–252.
- Gácsér A, Stehr F, KröGer C, Kredics L, SchäFer W, et al. 2007. Lipase 8 affects the pathogenesis of *Candida albicans*. *Infect Immun.* 75: 4710–4718.
- Garnaud C, Champlébois M, Maubon D, Cornet M, Govin J. 2016. Histone deacetylases and their inhibition in *Candida* species. *Front Microbiol.* 7:1238.
- Geiss GK, Bumgarner RE, Birditt B, Dahl T, Dowidar N, et al. 2008. Direct multiplexed measurement of gene expression with color-coded probe pairs. *Nat Biotechnol.* 26:317–325.
- Grainha T, Jorge P, Alves D, Lopes SP, Pereira MA. 2020. Unraveling *Pseudomonas aeruginosa* and *Candida albicans* communication in coinfection scenarios: insights through network analysis. *Front Cell Infect Microbiol.* 10:550505.
- Granger BL, Flenniken ML, Davis DA, Mitchell AP, Cutler LE. 2005. Yeast wall protein 1 of *Candida albicans*. *Microbiology* 151: 1631–1644.
- Haiko J, Saeedi B, Bagger G, Karpati F, Özenci V. 2019. Coexistence of *Candida* species and bacteria in patients with cystic fibrosis. *Eur J Clin Microbiol Infect Dis.* 38:1071–1077.
- Hnisz D, Bardet AF, Nobile CJ, Petryshyn A, Glaser W, et al. 2012. A histone deacetylase adjusts transcription kinetics at coding sequences during *Candida albicans* morphogenesis. *PLoS Genet.* 8: e1003118.
- Hnisz D, Majer O, Frohner I, Komnenovic EV, Kuchler K. 2010. The Set3/Hos2 histone deacetylase complex attenuates cAMP/PKA signalling to regulate morphogenesis and virulence of *Candida albicans*. *PLoS Pathog.* 6:e1000889.
- Hogan DA. 2002. *Pseudomonas-Candida* Interactions: An Ecological Role for Virulence Factors. *Science.* 296:2229–2232.
- Hogan DA, Vik A, Kolter R. 2004. A *Pseudomonas aeruginosa* quorum-sensing molecule influences *Candida albicans* morphology. *Mol Microbiol.* 54:1212–1223.
- Holcombe LJ, McAlester G, Munro CA, Enjalbert B, Brown AJ, et al. 2010. *Pseudomonas aeruginosa* secreted factors impair biofilm development in *Candida albicans*. *Microbiology* 156:1476–1486.
- Kim D, Perteza G, Trapnell C, Pimentel H, Kelley R, et al. 2013. TopHat2: accurate alignment of transcriptomes in the presence of insertions, deletions and gene fusions. *Genome Biol.* 14:R36.
- Kim T, Xu Z, Clauder-Münster S, Steinmetz LM, Buratowski S. 2012. Set3 HDAC mediates effects of overlapping non-coding transcription on gene induction kinetics. *Cell* 150:1158–1169.
- Lan C-Y, Newport G, Murillo LA, Jones T, Scherer S, et al. 2002. Metabolic specialization associated with phenotypic switching in *Candida albicans*. *Proc Natl Acad Sci USA.* 99:14907–14912.
- Lewis KA, Baker AE, Chen AI, Harty CE, Kuchma SL. 2019. Ethanol decreases *Pseudomonas aeruginosa* flagellar motility through the regulation of flagellar stators. *J Bacteriol.* 201:e00285-19. [10.1128/JB.00285-19]
- Li H, Handsaker B, Wysoker A, Fennell T, Ruan J, et al. 2009. The sequence alignment/map format and SAMtools. *Bioinformatics* 25: 2078–2079.

- Łoboda D, Rowińska-Żyrek M. 2017. Zinc binding sites in Pra1, a zincophore from *Candida albicans*. *Dalton Trans.* 46:13695–13703.
- Love MI, Huber W, Anders S. 2014. Moderated estimation of fold change and dispersion for RNAseq data with DESeq2. *Genome Biol.* 15:550.
- MacPherson S, Akache B, Weber S, De Deken X, Raymond M, et al. 2005. *Candida albicans* zinc cluster protein Upc2p confers resistance to antifungal drugs and is an activator of ergosterol biosynthetic genes. *Antimicrob Agents Chemother.* 49:1745–1752.
- Martchenko M, Alarco A-M, Harcus D, Whiteway M. 2004. Superoxide dismutases in *Candida albicans*: transcriptional regulation and functional characterization of the hyphal-induced SOD5 gene. *Mol Biol Cell* 15:456–467.
- McAlester G, O’Gara F, Morrissey JP. 2008. Signal-mediated interactions between *Pseudomonas aeruginosa* and *Candida albicans*. *J Med Microbiol.* 57:563–569.
- Mi H, Huang X, Muruganujan A, Tang H, Mills C. 2016. PANTHER version 11: expanded annotation data from Gene Ontology and Reactome pathways, and data analysis tool enhancements. *Nucleic Acids Res.* 45:D183–D189. [10.1093/nar/gkw1138]
- Mi H, Muruganujan A, Thomas PD. 2013. PANTHER in 2013: modeling the evolution of gene function, and other gene attributes, in the context of phylogenetic trees. *Nucleic Acids Res.* 41: D377–D386.
- Monteiro PT, Pais P, Costa C, Manna S, Sá-Correia I, et al. 2016. The PathoYeasttract database: an information system for the analysis of gene and genomic transcription regulation in pathogenic yeasts. *Nucleic Acids Res.* 45:D597–D603.
- Morales DK, Grahl N, Okegbe C, Dietrich LEP, Jacobs N, et al. 2013. Control of *Candida albicans* metabolism and biofilm formation by *Pseudomonas aeruginosa* phenazines. *mBio* 4:e00526-12.
- Morales DK, Hogan DA. 2010. *Candida albicans* interactions with bacteria in the context of human health and disease. *PLoS Pathog.* 6: e1000886.
- Neville BA, d’Enfert C, Bougnoux M-E. 2015. *Candida albicans* commensalism in the gastrointestinal tract. *FEMS Yeast Res.* 15: fov081.
- Nobile CJ, Fox EP, Hartooni N, Mitchell KF, Hnisz D, et al. 2014. A histone deacetylase complex mediates biofilm dispersal and drug resistance in *Candida albicans*. *mBio* 5:e01201-14.
- Polke M, Hube B, Jacobsen ID. 2015. *Candida* survival strategies. *Adv Appl Microbiol.* 91:139–235.
- Purschke FG, Hiller E, Trick I, Rupp S. 2012. Flexible survival strategies of *Pseudomonas aeruginosa* in biofilms result in increased fitness compared with *Candida albicans*. *Mol Cell Proteomics.* 11: 1652–1669. [10.1074/mcp.M112.017673]
- Quinlan AR, Hall IM. 2010. BEDTools: a flexible suite of utilities for comparing genomic features. *Bioinformatics* 26:841–842.
- Ramírez-Zavala B, Reuß O, Park Y-N, Ohlsen K, Morschhäuser J. 2008. Environmental induction of white-opaque switching in *Candida albicans*. *PLoS Pathog.* 4:e1000089.
- Schmieder R, Edwards R. 2011. Quality control and preprocessing of metagenomic datasets. *Bioinformatics* 27:863–864.
- Schofield DA, Westwater C, Warner T, Balish E. 2005. Differential *Candida albicans* lipase gene expression during alimentary tract colonization and infection. *FEMS Microbiol Lett.* 244:359–365.
- Sharek J, Belhumeur P. 2011. Modulation of morphogenesis in *Candida albicans* by various small molecules. *Eukaryot Cell* 10: 1004–1012.
- Singh RP, Prasad HK, Sinha I, Agarwal N, Natarajan K. 2011. Cap2-HAP complex is a critical transcriptional regulator that has dual but contrasting roles in regulation of iron homeostasis in *Candida albicans*. *J Biol Chem.* 286:25154–25170.
- Skrzypek MS, Binkley J, Binkley G, Miyasato SR, Simison M, et al. 2017. The *Candida* Genome Database (CGD): incorporation of assembly 22, systematic identifiers and visualization of high throughput sequencing data. *Nucleic Acids Res.* 45:D592–D596.
- Stacy A, McNally L, Darch SE, Brown SP, Whiteley M. 2016. The biogeography of polymicrobial infection. *Nat Rev Microbiol.* 14:93–105.
- Synnott JM, Guida A, Mulhern-Haughey S, Higgins DG, Butler G. 2010. Regulation of the hypoxic response in *Candida albicans*. *Eukaryot Cell* 9:1734–1746.
- Tao L, Du H, Guan G, Dai Y, Nobile CJ, et al. 2014. Discovery of a “white-gray-opaque” tristable phenotypic switching system in *Candida albicans*: roles of non-genetic diversity in host adaptation. *PLoS Biol.* 12:e1001830.
- Tillmann AT, Strijbis K, Cameron G, Radmaneshfar E, Thiel M, et al. 2015. Contribution of Fdh3 and Glr1 to glutathione redox state, stress adaptation and virulence in *Candida albicans*. *PLoS ONE* 10: e0126940.
- Trapnell C, Roberts A, Goff L, Pertea G, Kim D, et al. 2012. Differential gene and transcript expression analysis of RNA-seq experiments with TopHat and cufflinks. *Nat Protoc.* 7:562–579.
- Trejo-Hernández A, Andrade-Domínguez A, Hernández M, Encarnación S. 2014. Interspecies competition triggers virulence and mutability in *Candida albicans*–*Pseudomonas aeruginosa* mixed biofilms. *ISME J.* 8:1974–1988.
- Ullmann BD, Myers H, Chirananand W, Lazzell AL, Zhao Q, et al. 2004. Inducible defense mechanism against nitric oxide in *Candida albicans*. *Eukaryot Cell* 3:715–723.
- Xu W, Solis NV, Ehrlich RL, Woolford CA, Filler SG, et al. 2015. Activation and alliance of regulatory pathways in *C. albicans* during mammalian infection. *PLoS Biol.* 13:e1002076.

Communicating editor: J. Berman